Michigan State University

National Superconducting Cyclotron Laboratory

CHAOTIC DYNAMICS AND FLUCTUATIONS

Invited talk at "Dynamical Fluctuations and Correlations in Nuclear Collisions," Aussois, France, March 16-20, 1992

DIMITRI KUSNEZOV, AUREL BULGAC and JOHN SLOAN

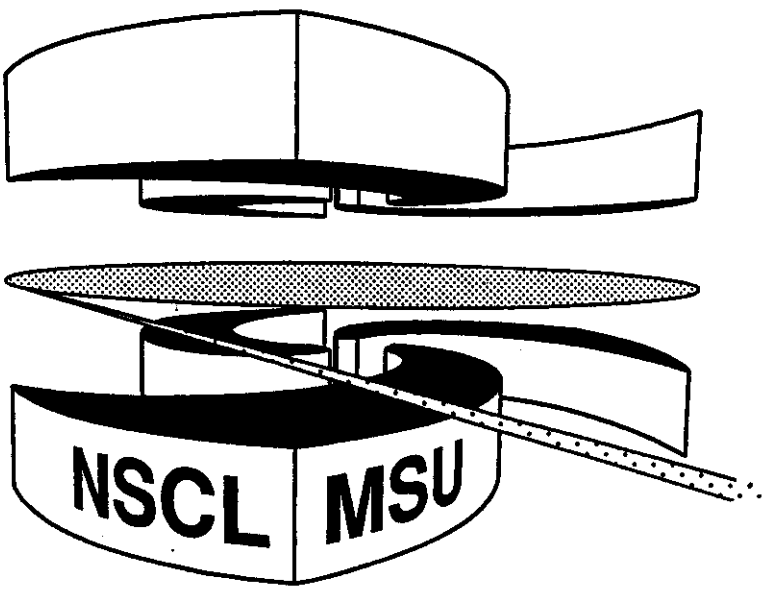

MSUCL-829 **MARCH 1992**

MSUCL-829
March, 1992

CHAOTIC DYNAMICS AND FLUCTUATIONS

Dimitri KUSNEZOV[a], Aurel BULGAC[b] and John SLOAN[c]

[a] Center for Theoretical Physics, Sloane Physics Laboratory Yale University, New Haven, CT 06511-8167, USA

[b] Department of Physics and Astronomy and National Superconducting Cyclotron Laboratory Michigan State University, East Lansing Ml 48824-1321, USA

[c] Department of Physics and Astronomy, Ohio State University, Columbus, OH 43210, USA

Abstract

A dynamical approach to the simulation of ensemble averages of complex systems can be realized by introducing new global degrees of freedom, called global demons. The role of the global demons is to render the dynamics chaotic, by coupling to the dynamical variables of the physical system in a particular manner and hence incorporating into these equations of motion the statistical propertles of the desired ensemble. The dynamic nature of the equations of motion allows one to investigate both equilibrium and non-equilibrium situations. These methods have the advantage of incorporating the symmetries of a problem into the equations of motion in a simple manner. The global character of the demons seems to be at the origin as well of a better handling of the critical slowing down phenomenon near phase transitions. The global demon approach is likely to have advantages when dealing with systems at finlte chemical potential (i.e. with complex actions), some aspects of fermionic theories, as well as (lattice regularized) field theory.

1. REMARKS ON STOCHASTIC FLUCTUATIONS

Many if not all of the current approaches to fluctuations in nuclear collisions are stochastic based algorithms. For example, one of the aims, which remains a fundamental problem, is how to evaluate the n-particle density $f_n(q_1, \ldots . q_n, p_1, \ldots, p_n)$ in a nuclear collision. Since no one has any idea how to compute f_n in practice, one usually integrates out n − 1 degrees of freedom and uses the one particle distribution:

$$f_1(q_1, p_1, t) = \int dq_2 \cdots dq_n dp_2 \cdots dp_n \, f_n(q_1, ..., q_n, p_1, ..., p_n). \quad (1)$$

The fluctuations of f_1 in nuclear collisions can now be studied in a variety of methods, such as implementing extended time-dependent Hartree-Fock with a Uehling-Uhlenbeck type collision term, the Vlasov-Boltzmann approach, the Boltzmann-Langevin (BL) equation and so forth[l]. This latter case typifies the approaches and for this reason it is useful to make a few superllcial

remarks here. The evolution of the one-body distribution in the BL method is governed by:

$$D[f_1] = \left[\frac{\partial}{\partial t} + v \cdot \nabla_q - \nabla_r U(f_1) \cdot \nabla_p\right] f_1 = K(f_1) + \delta K(q,p,t). \tag{2}$$

Since the collision term K cannot account for all the correlations, an additional stochastic term δK is added. While this is now a tractable problem, it is a severe truncation of the true situation in terms of removing correlations. While many n-particle distributions might have the same integrated f_1 in Eq. (1), they will have different higher moments f_2, f_3,... Hence while the Boltzmann equation gives a deterministic flow to f_1, the actual flow of f_1 should consist of many branches, each branch indicating the behaviour due to higher moments, and hence corresponding to different f_n's. This is the origin of δK. In the Boltzmann-Langevin approach, f_1 is treated as a stochastic variable and a distribution of f_1's is introduced. One assumption here is that the process can be characterized with Gaussian white noise:

$$\langle \delta K(q,p,t) \delta K(q',p',t') \rangle = C(q,p,q',p') \delta(t-t'). \tag{3}$$

This now becomes precisely a Brownian motion problem in distribution space, and there is a corresponding fluctuation dissipation theorem. The friction here is essentially the collision term, since it brings the system to equilibrium. A natural question arises here. While the 'true' dynamics of f_n (from the Liouville equation) is both deterministic and time-reversible, the BL equation in neither. So can it provide an accurate portrayal of the physics? One might also ask whether the white noise condition (3) is necessarily better than colored noise, and whether it is suited to phase transitions in which the energy distribution is bimodal (see below), rather than gaussian near the maximum. The analogy between the BL and Brownian motion is obvious:

$$m\dot{v} = -\gamma v + f(t), \qquad (\text{'particle} - \text{theory'}) \tag{4}$$

$$D[f_1] = K(f_1) + \delta K(q,p,t) \qquad (\text{'field} - \text{theory'}) \tag{5}$$

One of the main observations is that (4) corresponds to a distribution of particles, while (5) to a distribution on f_1's, and is essentially the study of a field theory. In what we describe below, the global demon approach is still closer to the particle limit (4) than to the field theory (5). In Section 3, extensions to field theory are proposed and studied, although not in the same context as (5). The fundamental difference between global demons and these stochastic approaches is that in the former, fluctuations are introduced *deterministically* with chaos rather than stochastically.

2. GLOBAL DEMON DYNAMICS

2.1 Survey of Simulation Techniques

The traditional dynamical approach to simulating densities $f(q,p)$ is molecular dynamics (MD), in which Hamilton's equations of motion are evolved in time, and the hydrodynamic flow naturally satisfies probability conservation. If the system is sufficiently large, or the interactions sufficiently complex, one usually imposes a quasi-ergodic hypothesis, and trusts that the Lyapunov instability is large enough for the simulation to converge to the proper ensemble. The alternative to deterministic algorithms is to use probabilistic algorithms based on Monte Carlo (MC). The drawback is the diffusive nature of the resulting 'dynamics' can often be too slow for many applications. So while MD evolves quickly through phase space, it is not ergodic, and while MC is ergodic, it is not fast. This has led to the development

of hybrid algorithms which include components of both MD and MC: the hybrid molecular dynamics (HMD) and hybrid Monte Carlo (HMC) algorithms[2]. Common to both HMC and HMD is the time evolution of Hamilton's equations of motion over some period of time T, followed by a momentum refresh. In the momentum refresh, all momenta are replaced with new (gaussian-distributed) random momenta, and then the simulation continued from the new point in phase space. One essential difference between HMD and HMC is that HMC is exact: it corrects HMD for the finite dt errors obtained while integrating the equations of motion. This is done by making a global Metropolis update at the end of the molecular dynamics component. By adding this acceptance probability, the dt errors associated with the time evolution average away to zero.

In contrast, global demons are a very general approach to simulating partition functions, using only dynamical equations of motion. These methods, based on an elegant proof by Nosé[3] and some inspirational equilibrium and non-equilibrium studies by Hoover[4], have been developed theoretically for a variety of physical situations[5]. The difference with MD is that the global demon formulation has nothing to do with Hamiltonian dynamics. For example, it can be defined completely in terms of coordinates alone if so desired. This is in contrast to MD and the hybrid algorithms, where a partition function whose action depends only on coordinates is usually augmented to included fictitious, or unneeded conjugate momenta in order to define a Hamiltonian or symplectic structure. One then uses Hamilton's equation of motion to define the dynamics. Another way to say this is that while Hamiltonian dynamics describes a microcanonical ensemble, the global demon dynamics describes a generic statistical ensemble. The global demon equations of motion are designed to evolve through the entire configuration space (it is *not* a phase space) such that the trajectory fill space with a density designed to reproduce the envisaged ensemble. Since it does not include any Monte Carlo step, the diffusive component present in the hybrid and other stochastic algorithms is absent here.

2.2 Global Demons

Let us consider a system characterized by an action $S(x)$ and coordinates $x = (x_1, ..., x_n)$. The ensemble averages of this system will have the generic form

$$\langle \mathcal{O} \rangle = \frac{1}{Z} \int \mathcal{D}\mu(x)\, e^{-\beta S(x)} \mathcal{O}, \qquad Z = \int \mathcal{D}\mu(x)\, e^{-\beta S(x)}. \tag{6}$$

Z is the normalization, and the measure $\mathcal{D}\mu(x)$ might include constraints (for example, symmetries associated with a Lie algebra). In this article, we are only concerned with the situation when the measure is $\mathcal{D}x$. A discussion of more general measures can be found in Ref. [6]. In what is more or less standard practice, conjugate momenta are introduced and added to $S(x)$ to make the exponent in (6) resemble a Hamiltonian (when they are not already present):

$$H(p, x) = \frac{1}{2} \sum_{i=1}^{n} p_i^2 + S(x), \tag{7}$$

and the measure is modified to $\mathcal{D}x\mathcal{D}p$, with appropriate normalization. Molecular dynamics is then easily implemented, and leads to the equation of motion

$$\dot{x}_i = p_i\,, \qquad \dot{p}_i = -\frac{\partial S(x)}{\partial x_i}, \qquad (i = 1, ..., n), \tag{8}$$

which preserve the energy $H(p, x)$.

In contrast, let us define a very general dynamics only in terms of the coordinates:

$$\dot{x}_i = -\frac{\beta}{n} \sum_{\alpha=1}^{m} \kappa_\alpha\, g_\alpha(w_\alpha)\, F_{\alpha i}(x)\,, \qquad (i = 1, ..., n). \tag{9a}$$

Here $g_\alpha(w_\alpha)$ and $F_{\alpha i}(x)$ are arbitrary functions of the global demon variables w_α and coordinates x, respectively, and κ_α are coupling constants. The number of global demon interactions in (9a) is unrestricted, but $\alpha = 2$ or 3 is usually sufficient. Notice that $\dot{x}$ does not depend explicitly on the Hamiltonian. An alternative formulation of the dynamics which includes a relic of the underlying Hamiltonian $H(p,x)$ is

$$\dot{x}_i = p_i - \frac{\kappa_1 \beta}{n}\, g_1(w_1)\, F_{1i}(x) \tag{9b}$$

$$\dot{p}_i = -\frac{\partial S(x)}{\partial x_i} - \frac{\kappa_2 \beta}{n}\, g_2(w_2)\, F_{2i}(p), \tag{9c}$$

An important observation here is that while we can retain a Hamiltonian sub-structure to the dynamics, it is not responsible for the ergodicity in the full configuration space, and can be retained or altogether removed (of course this will have some effect on the convergence)[7]. In non-equilibrium simulations, it is more convenient however, to use (9b-c) since there is a closer link to the thermodynamics of $H(p,x)$. Eqs. (9b-c) also have a microcanonical limit when $\kappa_\alpha = 0$. For the moment we retain the momenta in order to have a greater parity between this and other dynamical algorithms. In any case, the results below are independent of which form we take.

With the introduction of the global demons w_α, a larger configuration space $\{\phi\}$ must be defined, where $\phi = (x_1, ..., p_n, w_1, ...w_m)$ (or $\phi = (x_1, ..., x_n, w_1, ...w_m)$ if we use (9a)). In $\phi-$space we can define a new action f, which is determined by the equations of motion (9) in a natural way:

$$f(x,p,w) = S(x) + \frac{1}{2}\sum_{i=1}^{n} p_i^2 + \sum_{\alpha=1}^{m} \int_0^{w_\alpha} dw'_\alpha\, g_\alpha(w'_\alpha). \tag{10}$$

Unlike $H(p,x)$ in molecular dynamics, f is *not* preserved by the equations of motion. While the definition of f is not unique, it is natural as well as convenient in determining the dynamics of the global demons, by providing a particular solution to the continuity equation below. Eq. (10) defines the $\phi-$space measure as $\mathcal{D}x\mathcal{D}p\mathcal{D}w \exp(-\beta f)$. The global demon dynamics can then be determined by requiring that $\rho_f = \exp(-\beta f)$ be a stationary solution of a generalized continuity equation in configuration space:

$$0 = \frac{\partial \rho_f}{\partial t} + \sum_{i=1}^{n+m} \frac{\partial(\dot{\phi}_i \rho_f)}{\partial \phi_i}. \tag{11}$$

This is equivalent to the requirement that the master equation enforcing conservation of probability be satisfied.

The global demon equations of motion are then defined by requiring that the generalized dynamics of (9) preserve the desired measure (10). A direct substitution of ρ_f and $\dot{\phi}_i$ (Eqs. (9b-c)) into (11), and solving for $\dot{w}$ gives:

$$\dot{w}_\alpha = \frac{\kappa_\alpha}{n}\left(\beta F_{\alpha i}(x)\frac{\partial S(x)}{\partial x_i} - \frac{\partial F_{\alpha i}(x)}{\partial x_i}\right), \qquad (\alpha = 1, ..., m). \tag{12}$$

If we had chosen to neglect the momenta and used (9a), the form of Eq. (12) would be unchanged. So Eqs. (9) and (12) defines a dynamics which by construction preserves the measure (10). (It is worth noting that while we have taken an exponential form for the density, in general we can take an arbitrary function ρ and still use this same procedure.)

At the moment there seems to be a lot of freedom in defining the dynamics: $g_\alpha(w_\alpha)$, $F_{\alpha i}(x)$ and κ_α. The only restriction on $g_\alpha(w_\alpha)$ is that the measure (10) is normalizable. Although this does not place much restriction on the functional form of $g_\alpha(w_\alpha)$, a highly non-linear function will require a very small integration time step. For these reasons, it is convenient to take $g_\alpha(w_\alpha) = w_\alpha$ or $g_\alpha(w_\alpha) = w_\alpha^3$. The only restriction on $F_{\alpha i}$ is that the ultimate term in (12) be non-vanishing. So the functions $F_{\alpha i}$ must be at least linear in their argument. These terms are related to the divergence of the equations of motion, and their derivatives determine the rate of breathing of a volume V in configuration space, or equivalently, the instantaneous $\phi-$space compressibility. By application of the divergence theorem

$$\frac{dV}{dt} = -\frac{\beta}{n}\int_V \mathcal{D}\phi \left(\kappa_1 g_1(w_1)\frac{\partial F_{1i}}{\partial x_i} + \kappa_2 g_2(w_2)\frac{\partial F_{2i}}{\partial p_i}\right), \tag{13}$$

In the microcanonical limit, $\kappa_i = 0$, and $dV/dt = 0$ as required.

In conventional simulations, the change in action between measurements $\Delta S = S(\phi_2) - S(\phi_1)$ is usually related to the acceptance probability, and a small value is desired. In the global demon method, a trajectory should fill configuration space as rapidly as possible, and a large ΔS is needed:

$$\Delta S \simeq \Delta t \frac{\partial S}{\partial \phi_i}\dot{\phi}_i = -\frac{\beta}{n}\left(\kappa_1 g_1(w_1)\frac{\partial F_{1i}}{\partial x_i} + \kappa_2 g_2(w_2)\frac{\partial F_{2i}}{\partial p_i}\right). \tag{14}$$

If two points along a trajectory, ϕ_1 and ϕ_2, were truly decorrelated, $\sigma = \sqrt{\langle \Delta S^2 \rangle}$ would simply be related to the total specific heat of the system C_t,

$$\sigma_u = \sqrt{2(\langle S(\phi)^2\rangle - \langle S(\phi)\rangle^2)} = \frac{1}{\beta}\sqrt{2C_t}. \tag{15}$$

It is interesting to compare the ratio of σ to σ_u to see how large the steps are through configuration space. Near phase transitions where C_t increases rapidly, critical slowing down can be investigated by measuring σ and σ_u and plotting their ratio.

2.3 Density of States and Thermodynamics

One can extract a variety of information from such simulations. As an example, one can compute densities of states (up to normalization), of which entropy, the free energy and specific heat are only a few of the measurable quantities which are useful in the investigation of phase transitions. Some details with applications are in [8]. Additional equilibrium and non-equilibrium quantities, such as diffusion constants, can be found in [4,3].

3. STUDIES AND EXTENSIONS

The global demon method has been extended to general measures and applied to a variety of physical problems. Here we outline some of these efforts.

3.1 Complex Probabilities

There are many situations when one encounters complex probabilities, such as in the study of fermions or in general for quantum systems via the path integral. When the action $S(x)$ in (6) is complex, there are several approaches one can pursue. Parisi introduced a complex Langevin

algorithm which has been attacked both classically and quantum mechanically[9]. When one complexifies these and other standard algorithms, one invariably encounters trajectories which are unbounded in some direction of the complex plane, leading to instabilities. One way to avoid this is by writing the action $S(x) = S_r(x) + iS_i(x)$, where $S_r(x) = Re[S(x)]$ and $S_i(x) = Im[S(x)]$. The real part of the action $S_r(x)$ then defines the ensemble. The expectation of an operator $\mathcal{O}$ in the S (complex) ensemble is then written as

$$\langle \mathcal{O} \rangle_S = \frac{\int d\mu[x] e^{-S_r(x)} \left(e^{-iS_i(x)} \mathcal{O} \right)}{\int d\mu[x] e^{-S_r(x)} \left(e^{-iS_i(x)} \right)} = \frac{\langle \mathcal{O} e^{-iS_i(x)} \rangle_{S_r}}{\langle e^{-iS_i(x)} \rangle_{S_r}} \tag{16}$$

Here $\langle \rangle_{S_r}$ indicates the ensemble average in the real ensemble. Notice that all expectation values are with real probabilities, and the application of global demons is trivial. A typical action than one often encounters in field theory is essentially of the form $S = \sigma x^2 + x^4/2$, where $\sigma = \sigma_r + i\sigma_i$ [9]. The time dependence of $\langle x^2 \rangle$ in this measure is indicated in Fig. 1 for $\sigma = 2 + 2i$. The ratio of the expectation value of the full measure S to the expectation of S_r indicates the degree of cancelation due to the phase $\exp(-iS_i)$, and is $\sim 12\%$ for this case. The larger the cancelation, the longer it takes to thermalize. Details can be found in [10].

3.2 Phase Transitions in Molecules and Nuclei

We have studied phase transitions in alkalia-metal clusters, in particular $Na_{7,8,9}$. The Na_8 cluster is of special interest since its magic structure (due to electronic shell closure) provides enhanced stability and hence a high experimental production rate[11]. The strong delocalization of the valence electrons can then be imitated by a many-body potential, which is easily simulated in the Born-Oppenheimer approximation. In spite of the relatively small number of particle in a microcluster its properties are rather complex[8]. One of the most spectacular features is the coexistence of liquid and solid phases and the occurrence of phase transitions. In Fig. 2 the specific heat (for the potential energy U only) for the Na clusters is shown. One can see the presence of two peaks, a smaller, less defined one around 200 K, corresponding to a solid-glass phase transition, and a larger one around 700-1000 K, corresponding to the glass-liquid phase transition of these clusters. From the runs at about ten different temperatures, ranging from 25 to 1500 K we extracted the density of states (here for the potential energy only) in a rather wide range of excitation energies of the cluster, see Fig. 3. In each run we had 10^6 "measurements" (the total time of the trajectory between 200 psec for high T and 2000 psec for low T). One million configurations allowed us to define the density of states over essentially twelve orders of magnitude, in an energy interval around the average $U(T)$. By piecing together different portions of $\rho(U)$ we defined the density of states with quite high accuracy for over more than 20 orders of magnitude. The knowledge of the density of states allows one to predict the thermal behaviour of the system. In contradistinction to an infinite system, the phase transitions are not sharp, however, they are quite well defined and amenable to observation. The distribution of (potential) energy can have a double-humped structure at temperatures around the phase transition, see Fig. 4.

An interesting application of global demons to compact manifolds is the case of collective motion of nuclei. The Lipkin-Meshkov-Glick Hamiltonian is an example of $SU(3)$ symmetry:

$$\hat{H}_{LMG} = \sum_{k=1}^{3} E_k \left(\sum_{m=1}^{M} a_{km}^{\dagger} a_{km} \right) - \frac{1}{2} \sum_{k,l=1}^{3} V_{kl} \left(\sum_{m=1}^{M} a_{km}^{\dagger} a_{lm} \right)^2 , \tag{17}$$

where a_{kl} ($a_{kl}^{\dagger}$) annihilates (creates) particle l in level k. One particularly interesting limiting form is

$$H = \frac{V}{12} \left[8Q^2 + \frac{3}{2} L^2 \right] , \tag{18}$$

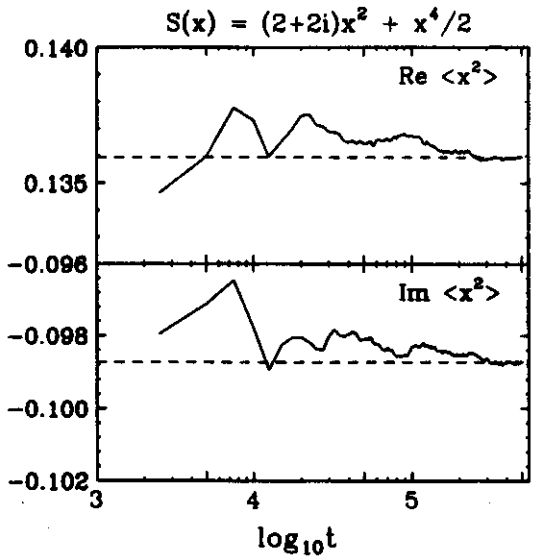

Figure 1. Time evolution of the real and imaginary parts of $\langle x^2 \rangle$ in the complex measure with $\sigma = 2 + 2i$. Dashed line is the exact result.

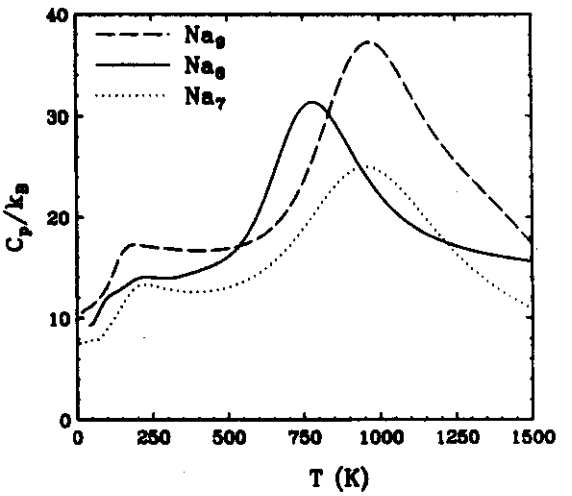

Figure 2. Specific heat for the potential energy for $Na_{7,8,9}$ clusters, computed from the density of states.

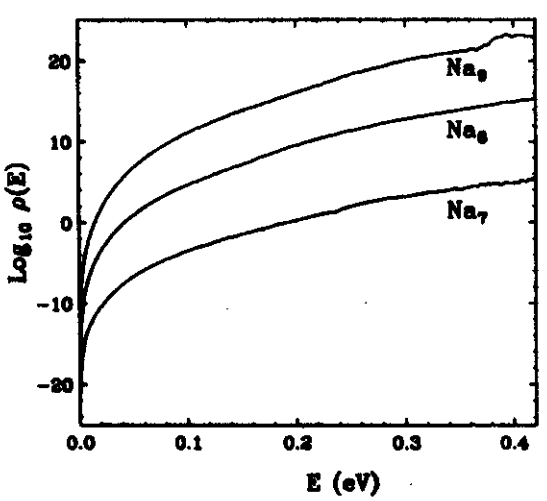

Figure 3. Contribution to the density of states from the potential energy for $Na_{7,8,9}$ clusters. The energy is the energy per atom, and problems with low statistics can be seen for $E \sim 0.4eV$.

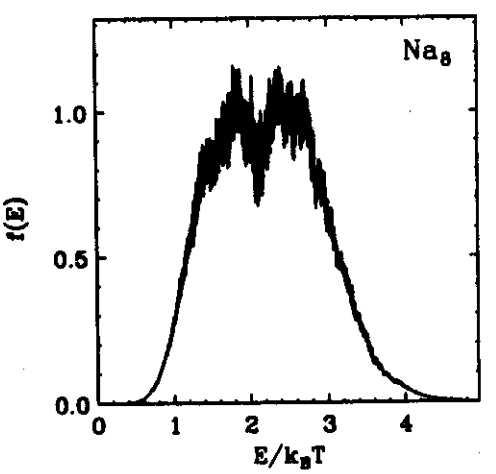

Figure 4. The distribution of the potential energy at $T = 820K$ for Na_8. The bimodal structure is characteristic of the phase transitions in microclusters and corresponds to the coexistence of a glassy and liquid phase.

where Q and L are the quadrupole and angular momentum generators of $SU(3)$. This is a crude model for nuclear collective excitations. The statistical properties of this model can be studied easily[6]. The energy distributions $f(E)$ for $T = 1$ and $T = 0.1$ are shown in Fig. 5, indicating a change in structure between these temperatures. In Fig. 6 we address the question of how many global demons one should include in (9), by comparing the results of $SU(3)$ simulations using two and three global demons. The dotted line corresponds to the two global demon ($N = 2$) case discussed above with $T = 0.1$. The solid line corresponds to the addition of the third global demon. As one can see, the additional global demon significantly improves the rate of thermalization. The equilibrium value of $< E >$ corresponds to the mean of the distribution $f(E, T = 0.1)$ in Fig. 5.

3.3 Quantum Systems and Path Integrals

There are many ways one can think of approaching quantum simulations, which might involve: using the density matrix formalism, path integrals, direct application of the Schrödinger equation, time evolution of Slater determinants, and so forth. Here we would like to mention two of the myriad of possibilities. For example, the Schrödinger equation for a finite dimensional Hilbert space can be written in terms of its matrix elements, after which it resembles Hamilton equations of motion. As such, it can be simulated dynamically. One obtains a non-linear Schrödinger equation which generates ergodic wavefunctions. One can envision the ergodic wavefunction as a wavefunction which 'rotates' through Hilbert space as it evolves in time such that ($\hat{\mathcal{O}}$ is an arbitrary operator)

$$\frac{1}{t}\int_0^t dt' \langle \Phi(t') \mid \hat{\mathcal{O}} \mid \Psi(t') \rangle \propto \frac{\mathrm{Tr}(\hat{\rho}\hat{\mathcal{O}})}{\mathrm{Tr}(\hat{\rho})}. \tag{19}$$

Such wavefunctions can be generated, as shown in Fig. 7 for the Hamiltonian $H = \hat{\sigma}_z$. The convergence of the left hand side of (28) to the exact result is indicated in Fig. 8. One of the drawbacks of this approach is that is requires some knowledge of the density matrix in order to solve for the dynamics. It is likely that one can devise completely different approaches as well, by modifying the time dependent Schrödinger equation through the addition of a properly chosen "random" field and/or making it nonlinear and/or relinquishing the hermiticity of the Hamiltonian. This class of modifications of the Schrödinger equation are then in the same spirit as the modifications of the classical Hamilton equations of motion we described earlier. On the other hand, this method as it stands allows one to study non-equilibrium quantum phenomena in cases where $\hat{\rho}$ is known.

Another approach is via the path integral. Writing the quantum partition function as a path integral, one can directly apply global demon techniques. For Hamiltonians in ordinary phase space, one obtains a path integral in q and p with a complex action. But since the momenta enter as gaussian variables, they can be integrated out leaving a real action. Simulation of 1-d harmonic oscillators where the results are known and Ne_2 in a Lennard-Jones 6-12 potential have been investigated. On the other hand, if one considers the path integral for a spin, there are no longer global definitions of coordinate and momenta, and as a result, the action is not only complex, but a nonlinear function of coordinates and momenta. For many body systems, one is also faced with symmetrization problems, and in general the path integral approach becomes very cumbersome. It is clear that new approaches to quantum simulations are needed.

3.4 Field Theories: Lattice Regularized Models

One of the drawbacks of hybrid Monte Carlo (HMC) is that it suffers from critical slowing down, i.e. the autocorrelation time τ for successive measurements to decorrelate goes like $\tau = \alpha\xi^z$, where ξ is the correlation length of the system and z is the dynamical critical exponent.

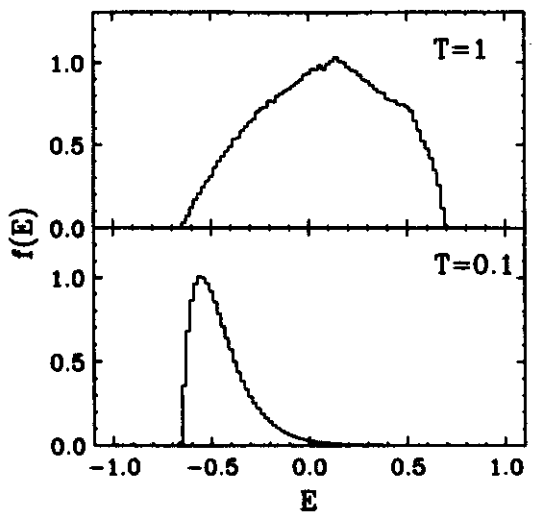

Figure 5. Energy distribution $f(E)$ for collective nuclear excitations (Eq. 18) at $T = 1$ and $T = 0.1$. $f(E)$ is obtained by histogramming the value of H at every point along the trajectory.

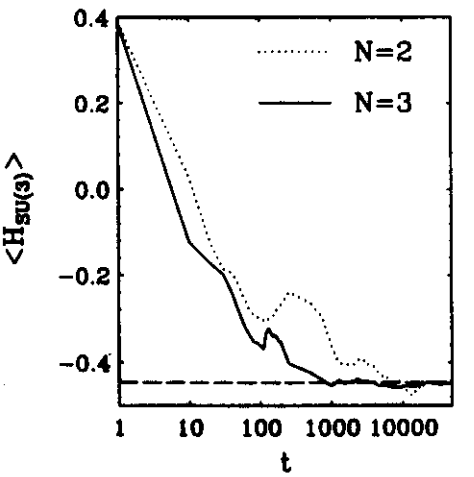

Figure 6. Comparison of convergence using two and three global demons for an $SU(3)$ Hamiltonian. Thermalization can be seen to improve with additional global demons.

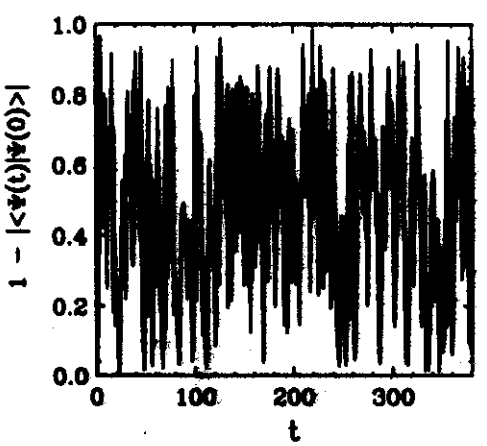

Figure 7. An ergodic wavefunction generated from a non-Hermitian Schrödinger equation. The intial state if spin up $\Psi(t = 0) = \uparrow$, and the time dependence of the projection of $\Psi(t)$ on $\Psi(0)$ is plotted.

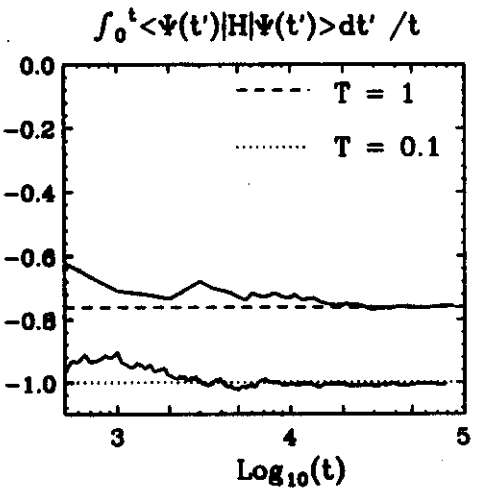

Figure 8. Verification of the quantum ergodicity condition (19). The exact results are broken lines (rhs of (19)) and the solid line is the lhs of (19). The wavefunction can be seen to be ergodic.

Near phase transition where $\xi \to \infty$, simulations can simply be impossible, hence algorithms with a small prefactor α and exponent z can make a tremendous difference. It has been shown that HMC simulations of free field theory will have z ranging between 1 and 2, depending on the time T between momentum refreshes. In the limit $T \to 0$, the HMC algorithm becomes a Langevin algorithm, and $z = 2$, as is typical for diffusive systems. When T is proportional to the period of the lowest frequency mode in the system, then $z = 1$ [12]. This means that in order to obtain optimum performance, a fine tuning of T is required, which depends on knowledge of the system being simulated. In contrast, global demons require little or no tuning near phase transitions, and unlike these algorithms which can never be better than $z \sim 1$ because they are local[13], global demons are global and presumably do not have the same limitations.

We have studied the 2D XY model, a lattice spin model, which has an infinite order (Kosterlitz-Thouless) phase transition near $\beta = 1$[14]. The dynamical critical exponent z was estimated and compared to state of the art algorithms: HMC, HMC-s which takes trajectory lengths of ξ, and HMC-1 which takes lengths of $2\pi\xi$. The action has the form

$$V(\theta) = -\sum_{<ij>} \cos(\theta_i - \theta_j), \tag{20}$$

where the sum is over nearest neighbors. In Fig. 9 we compare results for the auto-correlation functions for total lattice magnetization at the representative temperatures $\beta = 4.0$, $1/1.04$, 0.7, with several variations of HMC. The global demon approach can be seen to decorrelate much faster than the HMC based approaches. In Fig. 10 we plot $\sqrt{\Delta S^2}/\sigma_u$ versus β on a 16^2 lattice. The simulation was performed with two global demons and hence two constants κ_1, κ_2. Measurements of ΔS were performed at time steps of length $T = 1$, using $dt = 0.1$ and leapfrog integration. What is seen is that as one increases the coupling strength of the global demons, the trajectory more efficiently diffuses through configuration space, and that there is a saturation when $\kappa_1 = \kappa_2 = 32 \sim o(16)$. The dip near $\beta = 1$ in Fig. 10 occurs near the (Kosterlitz-Thouless) phase transition, and is a manifestation of critical slowing down. But as one readily observes, the algorithm is not strongly affected, even though the correlation length of the system diverges exponentially. In this region, C_t increases quite rapidly, and the algorithm is able to compensate without additional tuning. Analogous features are found in the decorrelation times.

3.5 Non-Equilibrium Simulations

We shall only present an extension of the present ideology to the study of Brownian motion[5]. Almost anyone is familiar with the phenomenology of the Brownian motion in the Langevin description. The Newton equation of motion is modified by adding a dissipative term (friction) and a random force (usually white noise). Both these additional terms lead to an irreversible time evolution. There is a long standing argument on whether the equation of motion for a Brownian particle should have a dissipative and irreversible character; it does not seem that there is a consensus yet. In a way the presence of the two additional terms looks like overdoing things. The random force should account for whatever the surrounding molecules do to the Brownian particle and the friction term looks a bit superfluous. MD ideology should in principle be able to describe Brownian motion as well, especially if one intends to study transport and nonequilibrium phenomena. In Ref. 5 we have shown that one can develop a deterministic and time-reversal invariant description for a Brownian particle. Instead of the celebrated Langevin equation, global demons provide a time-reversal invariant deterministic set of equations. The deterministic "thermal" force exerted by the medium on the particle is illustrated in Fig. 11. As one can see, it looks pretty random. Namely this feature ensures that the rms radius of a particle (initially at the origin) behaves like $1/\sqrt{t}$ over long periods of time,

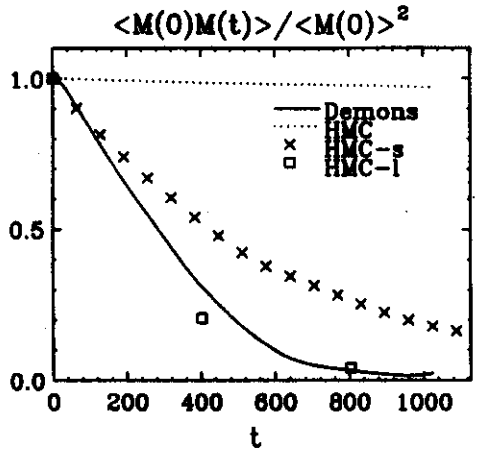

Figure 9. Auto-correlation function for the total magnetization of the 2D XY model on a 64^2 lattice at $\beta = 4$, computed with global demons and variations of HMC. The symbols indicate the actual time separation between measurements for HMC.

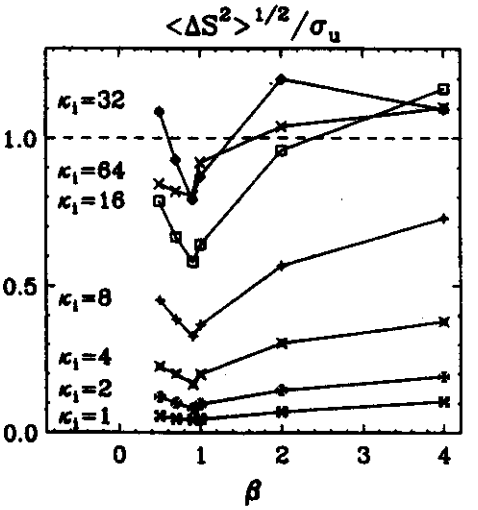

Figure 10. Dependence of the normalized rms change in action per time step along a global demon trajectory for the 2D XY model, as a function of β on a 16^2 lattice. Two global demons were used with equal coupling κ_i. The dip near $\beta = 1$ is a result of critical slowing down near the phase transition.

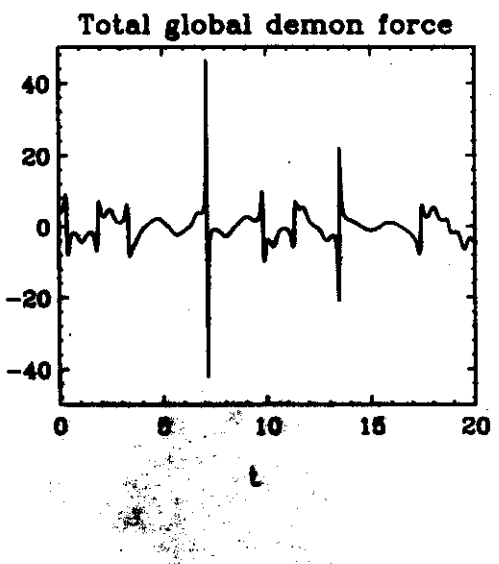

Figure 11. Characteristic behavior of the (deterministic) friction force $\dot{p} = F(t)$ for a Brownian particle.

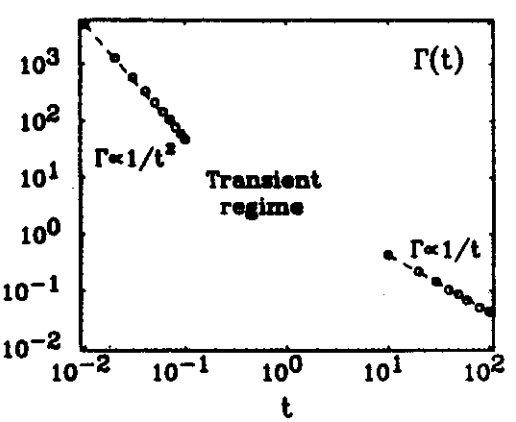

Figure 12. Time dependence of the inverse width of the distribution $f(q,t) = \sqrt{\Gamma(t)/\pi}\exp[-\Gamma(t)q^2]$ using time reversible deterministic dynamics. The mean spreading velocity reaches the Brownian limit $\sqrt{t}$ for long times.

see Fig. 12. At the same time, the momentum has an Boltzmann distribution as expected for a Brownian particle. We find it remarkable that a diffusion process can be described without any recourse to dissipation (time irreversibility) and/or random noise (non-deterministic element).

But perhaps the most striking work is that by W.Hoover and his collaborators. In their work they have investigated a variety of non-equilibrium situations, finding strange attractors in phase space. Many of these details can be found in [7].

4. CONCLUSIONS

We have outlined some of the directions of global demons. But in some sense we are still at the level of particles (Eq. (4)) rather than fields (Eq. (5)). The theoretical foundations of global demons seem to be much broader than previously thought, and there is much room for development. What is interesting is the rather remarkable simplicity with which one can obtain very detailed information about complex systems both in and out of equilibrium.

Support was provided under DOE grants DE-FG02-91ER40608, DE-AC02-ER01545 and NSF Grant No. 89-06670.

5. REFERENCES

1. S.Ayik and C.Gregoire, Phys. Lett. **212B** (1988) 269; Nucl. Phys. **A513** (1990) 189; J.Randrup and B.Rémaud, Nucl. Phys. **A514** (1990) 339; E.Suraud, S.Ayik, M.Belkacem and J.Stryjewski, Nucl. Phys. A (in press); V.R.Pandharipande and T.J.Schlagel, Illinois preprint ILL-NU-90-19 (1990).
2. S.Duane, A.D.Kennedy, B.J.Pendelton and D.Roweth, Phys. Lett. **B195** (1987) 216.
3. S.Nosé, Prog. Th. Phys. Suppl. **103** (1991) 1 and references therein; J.Chem.Phys. **81**, (1984) 511; Mol.Phys. **52** (1984) 255.
4. W.G.Hoover, *Computational Statistical Mechanics*, (Elsevier,New York, 1991) and references therein; W.G.Hoover, A.Ladd and B.Moran, Phys.Rev.Lett. **48** (1982) 1818.
5. A.Bulgac and D.Kusnezov, Phys. Rev. **A42**, 5045 (1990); Phys. Lett. **A151** (1990) 122; D.Kusnezov, A.Bulgac and W.Bauer, Ann. Phys. **204**, 155 (1990).
6. D.Kusnezov and A.Bulgac, Ann. Phys. (NY) **214** (1992) 180; D.Kusnezov, Yale University preprint YCTP-N38-91 (1992), submitted.
7. D.Kusnezov, Yale University preprint YCTP-N39-91 (1992), submitted.
8. A.Bulgac and D.Kusnezov, Phys. Rev. Lett. **68** (1992) 1335; Phys. Rev. **B45** (1992) 1988.
9. G. Parisi, Phys. Lett. **131B** (1983) 393; J. Ambjorn and S.K.Yang, Phys. Lett. **165B** (1985) 140; J. Klauder, Phys. Rev. **A29**, (1984) 2036; J. Klauder and W. Petersen, J.Stat.Phys. **39** (1985) 53.
10. D.Kusnezov, Yale University preprint YCTP-N6-92 (1992).
11. W.A.De Heer, W.D.Knight, M.Y. Chou and M.L. Cohen, in *Solid State Physics*, edited by H. Ehrenreich and D.Turnbull (Academic, New York, 1987), Vol. 40, p.93.
12. G. Bathas and H. Neuberger, Rutgers University preprint RU-91-46 (1991).
13. A.D.Kennedy and B. Pendelton, Nucl. Phys. (Proc. Suppl.) **B20** (1991) 118.
14. J.H.Sloan, D.Kusnezov and A.Bulgac, Yale preprint YCTP-N23-91, OSU preprint OSU-DOE-ER-1545-561 (submitted); D.Kusnezov and J.H.Sloan, Yale University preprint YCTP-N1-92 (1992) submitted.